

Environmental determinants of COVID-19 transmission across a wide climatic gradient in Chile

Francisco Correa-Araneda (✉ francisco.correa@uautonoma.cl)

Unidad de Cambio Climático y Medio Ambiente, Instituto de Estudios del Hábitat, Facultad de Arquitectura y Construcción, Universidad Autónoma de Chile, Temuco, Chile <https://orcid.org/0000-0001-6670-6661>

Alfredo Ulloa-Yañez

Unidad de Cambio Climático y Medio Ambiente, Instituto de Estudios del Hábitat, Facultad de Arquitectura y Construcción, Universidad Autónoma de Chile, Temuco, Chile

Daniela Núñez

Programa de Doctorado en Ciencias mención en Ecología y Biología Evolutiva, Facultad de Ciencias, Universidad de Chile, Chile

Luz Boyero

Department of Plant Biology and Ecology, Faculty of Science and Technology, University of the Basque Country (UPV/EHU), 48940 Leioa, Spain <https://orcid.org/0000-0001-7366-9299>

Alan M. Tonin

Aquariparia/Limnology Lab, Department of Ecology, IB, University of Brasília (UnB), Brasília, Brazil <https://orcid.org/0000-0002-8463-8823>

Aydeé Cornejo

Freshwater Macroinvertebrate Laboratory. Zoological Collection Dr. Eustorgio Mendez, Gorgas Memorial Institute for Health Studies (COZEM-ICGES), Ave. Justo Arosemena and Calle 35, 0816-02593, Panama City, Panama <https://orcid.org/0000-0001-6789-5847>

Mauricio Urbina

Department of Zoology, Faculty of Natural and Oceanographic Sciences, University of Concepción, P.O. Box 160-C, Concepción, Chile

María Elisa Díaz

Departamento de Ciencias Ambientales, Facultad de Recursos Naturales, Universidad Católica de Temuco, Temuco, Chile

Guillermo Figueroa-Muñoz

Department of Zoology, Faculty of Natural and Oceanographic Sciences, University of Concepción, P.O. Box 160-C, Concepción, Chile

Carlos Esse

Unidad de Cambio Climático y Medio Ambiente, Instituto de Estudios del Hábitat, Facultad de Arquitectura y Construcción, Universidad Autónoma de Chile, Temuco, Chile <https://orcid.org/0000-0002-1783-535X>

Keywords: SARS-CoV-2, climate, population size, infection rate, South America

DOI: <https://doi.org/10.21203/rs.3.rs-30393/v1>

License:  This work is licensed under a Creative Commons Attribution 4.0 International License.

[Read Full License](#)

Abstract

Several studies have examined the transmission dynamics of the novel COVID-19 disease in different parts of the world. Some have reported relationships with several environmental variables, suggesting that spread of the disease is enhanced in colder and drier climates. However, evidence is still scarce and mostly limited to a few countries, particularly from Asia. We examined the potential role of multiple environmental variables in COVID-19 transmission rates and patterns from February 23 to April 16 across 121 cities of Chile; this country covers a large climatic gradient ($\approx 40^\circ$ of latitude, $\approx 4,000$ m of altitude and 5 climatic regions, from desert to tundra), but all cities share their social behaviour patterns and regulations. Our results indicated that COVID-19 transmission in Chile was mostly related to 3 main climatic factors (mean temperature, relative humidity and wind speed) and population size. Transmission was greater in colder and drier cities (although wind modulated the effect of temperature) and when wind speed was higher; finally, transmission increased with population size. The results of this study support some previous findings about the main environmental and demographic determinants of COVID-19 transmission, which may be useful for decision-making and management of the disease.

Introduction

On the last day of 2019, a viral outbreak of unknown origin was detected in a seafood market in Wuhan City, Hubei Province, China¹. This virus, later named *severe acute respiratory syndrome coronavirus 2* (SARS-CoV-2; Coronaviridae) and responsible for the clinical disease known as COVID-19, has now spread around the globe and declared a pandemic by the World Health Organization (WHO) on March 12, 2020. To date (April 25, 2020), it has been detected in 210 countries, with about 2.6 million people infected and 180 thousand deaths worldwide². The global scale and severity of the impacts of this disease, despite being at an intermediate stage of development, is unprecedented, and studies have suggested that it might take more than a decade for the world to recover from its effects, both socially and economically³.

Upon appearance of COVID-19, several studies have examined the transmission dynamics of this disease⁴. While some have documented the route of transmission through human-to-human contact, others have examined the role that some environmental factors may play in facilitating the rate of spread of the disease through the analysis of temporal and spatial relationships of these factors with COVID-19 transmission rate. Most of these studies have reported a negative relationship between transmission rate and several proxies of temperature and humidity, suggesting that the disease spread is enhanced in colder and drier climates⁵⁻⁹. Other environmental variables have received less attention and results have been inconclusive or differed among countries. For example, one study reported an inverse relationship between COVID-19 transmission and wind speed in Iran¹⁰, while global studies have found no significant association between both variables^{11,12}. A negative relationship of the disease transmission with solar radiation has been reported in Iran¹⁰, and a positive relationship with the concentration of atmospheric pollutants was found in China¹³. Overall, and despite the rapid response of the scientific community to

understand the transmission of COVID-19, the role that environmental variables play in the disease dynamics remains an open question that requires further evidence across the world.

The goal of this study was to examine the potential role of multiple environmental variables in COVID-19 transmission rates and patterns in Chile. Environmental variation within Chile is unique due to the particular geography of this country, which includes an altitudinal range of $\approx 7,000$ m from the sea level to the top of Aconcagua mountain, and a $\approx 40^\circ$ latitudinal gradient that covers 6 climatic zones, including desert, semiarid, mediterranean, marine west coast, tundra and ice sheet. At the same time, population across the country shares a common social behaviour, and regulations are established by a single national authority, allowing the evaluation of environmental variables under relatively socio-economic conditions. We thus aim to provide information about COVID-19 transmission across a wide range of environmental variation within a single country that may help understanding the dynamics of this disease.

Results

Summary of study area characteristics and COVID-19 transmission data

Mean temperature varied between 10.9°C (tundra climatic region) and 17.7°C (desert); relative humidity, between 59% (desert) and 77% (marine south west); atmospheric pressure, between 859 mbar (desert) and 1002 mbar (marine south west); and wind speed, between 5 km h^{-1} (desert and marine south west) and 10 km h^{-1} (tundra) (Table 1). Absolute population size ranged from 13,334 inhabitants (El Carmen, mediterranean) to 645,909 inhabitants (Puente Alto, mediterranean) (Fig. 1; see Supplementary Table S1 online). The first registered COVID-19 infection case in Chile occurred on February 23, 2020; to date (April 16), more than 8,800 infected inhabitants and 100 deaths have been reported. The mean absolute number of weekly infections ranged from 0.125 (several cities) to 68.375 (Temuco, mediterranean), and the relative number of weekly infections from 0.00004 (Peumo, mediterranean) to 3.04 (El Carmen, mediterranean) (see Supplementary Table S1 online).

Relationship between COVID-19 and predictive variables

Our models revealed that population size had the greatest (positive) effect on absolute infection rate, followed by mean temperature (negative effect), relative humidity (negative effect) and wind speed (positive effect); a significant interaction between temperature and wind, however, indicated that their effects depended on each other (Table 2). Relative infection rate was affected by mean temperature and relative humidity, both variables showing negative effects (Table 2; Fig. 2).

Discussion

Our results demonstrate that COVID-19 infection rate in Chile to date has been linked to 3 main environmental variables (mean temperature, relative humidity and wind speed) and to population size. Firstly, we found a negative relationship between infection rate and mean temperature (modulated by

wind speed for absolute, but not for relative infection rate). Other studies have reported a similar relationship between atmospheric temperature and the transmission of COVID-19¹⁴⁻¹⁷ and other respiratory diseases such as SARS¹⁸. These findings are particularly concerning at present in the southern hemisphere, which is entering winter and therefore lower temperatures are expected in the coming months, which could drive an upsurge of the disease.

The negative relationship that we observed between infection rate and relative humidity is consistent with former evidence that high relative humidity reduces the COVID-19 viability^{19,20} and transmission rates^{7,21}. Similarly, high relative humidity has been reported to reduce the survival of the influenza virus²² and the incidence of this disease⁸. Environmental humidity can affect viral transmission through its interaction with respiratory droplets, which act as virus containers and can remain longer in dry air^{23,24}. Additionally, high humidity leads to inactivation of the viral lipid membrane, and consequently a decrease in the virus stability and transmission^{25,26}. This relationship of infection rate with humidity could explain the fact that up to March 22, 2020, 90% of COVID-19 cases have been recorded in non-tropical countries, with much fewer cases recorded from the tropics²⁷.

We found that wind speed favoured COVID-19 transmission, although the significant interaction with temperature makes the interpretation of wind effects difficult. Wind speed and direction have been highlighted as relevant variables in the transmission of infectious diseases, but often neglected²⁸. However, studies have been inconclusive about the potential role of wind in COVID-19 transmission. While a study carried out in Iran reported an inverse relationship between both variables¹⁰, studies conducted in China found no significant relationship^{11,12}. Our results suggest that higher wind speed can cause higher spreading of suspended particles through the air; this hypothesis could be tested in Chile in the coming months, as wind is expected to increase considerably during the autumn and winter²⁹.

Other studies have estimated that climatic variables can explain up to 18% of the variation in COVID-19 transmission¹². In our study, population size was the strongest predictor of absolute infection rate, most likely due to the direct relationship existing between the spatial proximity of people and transmission of diseases³⁰. This relationship is particularly concerning in the light of growing human population, which is projected to reach 9.8 billion inhabitants globally by 2050³¹. In Chile, a population of 21.6 million inhabitants is expected by 2050, with inhabitants > 64 years old exceeding 3 million (25% of the population)³². Moreover, atmospheric pollution is generally greater in more populated cities; in our study, for example, the concentration of PM10 and PM2.5 increased with population density ($r = 0.38$, $p < 0.001$ and $r = 0.15$, $p = 0.032$, respectively), although we did not include these data in our analyses because of the low sample size of available pollution data. Previous studies have indicated that air pollutants are risk factors for respiratory infection by carrying microorganisms and affecting human immunity^{13,33-35}, and have been reported a significant association of PM10 and PM2.5 with hospitalizations due to respiratory disease^{33,34,36}. These relationships are particularly concerning in Chile, where 12 cities have

been ranked among the 15 most polluted in South America, with the capital city Santiago being in 35th place worldwide³⁷.

In conclusion, our study shows that climate plays a key role in the transmission of COVID-19 in Chile, a country that comprises a particularly high variation of environmental conditions. Importantly, it is highly likely that climatic conditions expected for the coming months in the southern hemisphere (i.e., lower temperature, lower humidity and higher wind speed) can favour a higher disease transmission speed. Our study and others providing information about how climatic and demographic factors can influence the spread of the disease may serve as the basis for predictive models of COVID-19 transmission through space and time, which will be highly relevant to decision-making and management of the disease.

Materials And Methods

Study area

We examined data from 121 'communes' or cities in Chile, which are distributed across 4,200 km from north to south. Latitudes of our study area range from 17°S (Arica) to 56°S of latitude (Cabo de Hornos), and altitudes range from 8 m a.s.l. (Pacific Ocean coast) to 3,962 m a.s.l. (San Pedro de Atacama, Andean mountain range). The study area covers the following five climatic zones: (i) desert (17°30' - 26°00'S), (ii) semiarid (26°00'-32°00'), (iii) mediterranean (32°00'-39°00'), (iv) marine west coast (39°00' - 44°00'S) and (v) tundra (44°00' - 56°00'S); the only climatic zone excluded from the study was the ice sheet (located in the highest areas of the Andes mountain range) because of the absence of human population. In terms of macroclimates, ca. 41% of the country is temperate, 31% arid and the remaining 28% has a polar climate²⁹.

Chilean population is 19.11 million inhabitants, of which 51% are women and 49% men. Life expectancies are 83 (women) and 78 (men) years old; 68.7% of the population is between 15-64 years old and 11.9% over 65 years old. The 88% of inhabitants live in urban areas and the estimated international migration rate is 12 per thousand inhabitants. The 13% of the population belongs to indigenous or native groups; 80% Mapuche, 7% Aymara and 4% Diaguita³⁸. The population is aging as a result of the decline in fertility and the increased life expectancy³².

Chile has 16 administrative regions^{29,39}, of which the Metropolitana region concentrates the largest population (7.1 million inhabitants), followed by the Valparaíso region (1.8 million inhabitants). In contrast, the Aysén and Magallanes regions, located in the southern extreme of Chile, have the smallest population (<200,000 inhabitants). Inhabitants > 65 years old mainly inhabit the areas with mediterranean climate in the cities of Santiago, Valparaíso and Concepción, and correspond to 6.28% of the total employed inhabitants in the country⁴⁰. By 2050 it is projected that total population size reaches 21.6 million (i.e., an increase of 15.3% compared to 2020) under assumptions of birth and immigration surpassing mortality and emigration, with inhabitants > 65 years old predicted to exceed 3 million (25% of the population)³².

COVID-19 transmission data and predictive variables

We characterized the COVID-19 transmission in Chile from February 23 to April 16, 2020, based on two variables: (i) mean absolute infection rate (i.e., number of infected inhabitants per week), and (ii) mean relative infection rate (i.e., the former variable divided by population size). Data were obtained from official sources of the Government of Chile⁴¹. We extracted daily climatic data from the databases of 121 meteorological stations in Chile⁴² corresponding to cities with presence of COVID-19, for the same period; these data were averaged per week to make them comparable with variables quantifying the disease transmission. The climatic variables extracted were the following: average, maximum and minimum atmospheric temperature (°C); relative (%) and absolute (g m^{-3}) humidity, accumulated precipitation (mm), atmospheric pressure (mbar), ultraviolet solar radiation (Mj m^{-2}) and wind speed (km h^{-1}). Additionally, we obtained data for other relevant environmental, demographic and geographic variables as follows: air pollutant data, including particulate matter with aerodynamic diameter $\leq 10 \mu\text{m}$ (PM10) and $\leq 2.5 \mu\text{m}$ (PM2.5), obtained from a database of 30 air quality stations⁴³; and city area (km^{-2}), population size (ind), population density (ind km^{-2}), latitude (absolute degrees), longitude (absolute degrees) and altitude (m a.s.l.), obtained from CONAF⁴⁴ and IDE Chile⁴⁵.

Statistical analyses

We examined all pairwise relationships between predictive variables with Pearson correlation coefficients [pairs.panels function, *psych* package (Revelle, 2016); R statistical software⁴⁶, and discarded variables showing high correlations with others ($r > 0.5$) for further analyses. Air pollution data were also discarded due to the low sample size (i.e., 30 out of 121 cities for which epidemiological data were available). The retained variables were: average temperature (which was significantly correlated with maximum and minimum temperature, latitude, longitude and altitude), relative humidity (related to absolute humidity, accumulated precipitation, latitude, longitude and altitude), atmospheric pressure, wind speed and population size (see Supplementary Table S2 online).

We explored the effects of the predictive variables on absolute and relative COVID-19 infection rates through linear models and a backward model selection procedure, based on the Akaike Information Criterion (AIC)⁴⁷. Prior to running the models, we examined Cleveland dot and boxplots for each response variable, which revealed outliers for absolute (1 outlier) and relative (3 outliers) COVID-19 infection rates that were confirmed with Cook's distances (using the residuals of the final model) and removed; predictive variables were standardized to unit variance (z-scores). Additionally, validation of the model for absolute infection rate showed an increase of model residuals with population size (and thus a violation of parametric model assumptions), which was solved by including a power variance function structure in the model (varPower function using population size). The models were fitted using the gls function of the *nlme* R package⁴⁸.

Declarations

Data availability

The raw data was supplied as a Supplementary Information File.

Acknowledgements

Funding was provided by the Initiation Fondecyt project 11170390 to FCA. DN received a CONICYT-PFCHA/Doctorado Nacional/2019-21191862 scholarship. AC received a scholarship of the National Secretariat of Science, Technology and Innovation (SENACYT, Panama) and by the National Research System of Panama (SNI; doctoral student category).

We thank Francisco Encina, Demian Arancibia, Rodrigo Correa, Ministry of Science and Technology and Ministry of Health of the Government of Chile for information support in data search and comments. FCA dedicates this study to his grandmother -*Tencha*- for her constant support and inspiration.

Author contributions

Contributions

Conceptualization: F.C.A. and C.E. Formal analysis: F.C.A., A.U.Y, L.B, A.T. and C.E. Literature revision: F.C.A., A.U.Y and D.N. Data curation: A.U.Y and D.N. Visualization: F.C.A., A.U.Y, D.N and C.E. Wrote the manuscript: F.C.A. and L.B. All authors reviewed and edited the manuscript.

Competing Interests Statement

The authors declare no competing interests.

References

1. Sarkodie, S. A. & Owusu, P. A. Investigating the cases of novel coronavirus disease (COVID-19) in China using dynamic statistical techniques. *Heliyon* **6**, e03747, <https://doi.org/10.1016/j.heliyon.2020.e03747> (2020).
2. WHO. Coronavirus disease (COVID-19) Pandemic. Available at: <https://www.who.int/emergencies/diseases/novel-coronavirus-2019> (2020).
3. United Nations. Launch of Global Humanitarian Response Plan for COVID-19. Available at: <https://www.un.org/sg/en/content/sg/press-encounter/2020-03-25/launch-of-global-humanitarian-response-plan-for-covid-19> (2020).
4. Li, Q. *et al.* Early Transmission Dynamics in Wuhan, China, of Novel Coronavirus-Infected Pneumonia. *N. Engl. J. Med.* **382**, 1199–1207, <https://doi.org/10.1056/NEJMoa2001316> (2020).
5. Liu, J. *et al.* Impact of meteorological factors on the COVID-19 transmission: A multi-city study in China. *Sci. Total Environ.* **726**, 138513, <https://doi.org/10.1016/j.scitotenv.2020.138513> (2020).

6. Luo, W. *et al.* The role of absolute humidity on transmission rates of the COVID-19 outbreak. *medRxiv* <https://doi:10.1101/2020.02.12.20022467> (2020).
7. Ma, Y. *et al.* Effects of temperature variation and humidity on the death of COVID-19 in Wuhan, China. *Sci. Total Environ.* 138226, <https://doi.org/10.1016/j.scitotenv.2020.138226> (2020).
8. Park, J. E. *et al.* Effects of temperature, humidity, and diurnal temperature range on influenza incidence in a temperate region. *Influenza Other Respi. Viruses* **14**, 11–18, <https://doi.org/10.1111/irv.12682> (2020).
9. Shi, P. *et al.* The impact of temperature and absolute humidity on the coronavirus disease 2019 (COVID-19) outbreak - evidence from China. *medRxiv*, <https://doi:10.1101/2020.03.22.20038919> (2020).
10. Ahmadi, M., Sharifi, A., Dorosti, S., Ghouschi, S. J. & Ghanbari, N. Investigation of effective climatology parameters on COVID-19 outbreak in Iran. *Sci. Total Environ.* 138705, <https://doi:10.1016/J.SCITOTENV.2020.138705> (2020).
11. Chen, B. *et al.* Roles of meteorological conditions in COVID-19 transmission on a worldwide scale. *medRxiv* **11**, <https://doi.org/10.1101/2020.03.16.20037168> (2020).
12. Oliveiros, B., Caramelo, L., Ferreira, N. & Caramelo, F. Role of temperature and humidity in the modulation of the doubling time of COVID-19 cases. *medRxiv*, <https://doi.org/10.1101/2020.03.05.20031872> (2020).
13. Zhu, Y., Xie, J., Huang, F. & Cao, L. Association between short-term exposure to air pollution and COVID-19 infection: Evidence from China. *Sci. Total Environ.* **727**, <https://doi.org/10.1016/j.scitotenv.2020.138704> (2020).
14. Luo, Y. *et al.* Lagged Effect of Diurnal Temperature Range on Mortality in a Subtropical Megacity of China. *PLoS One* **8**, e55280, <https://doi.org/10.1101/2020.02.12.20022467> (2013).
15. Pinheiro, S. de L. L. de, Saldiva, P. H. N., Schwartz, J. & Zanobetti, A. Isolated and synergistic effects of PM10 and average temperature on cardiovascular and respiratory mortality. *Rev. Saude Publica* **48**, 881–888, <https://doi.org/10.1590/S0034-8910.2014048005218> (2014).
16. Ficetola, G. F. & Rubolini, D. Climate affects global patterns of COVID-19 early outbreak dynamics. *medRxiv*, <https://doi:10.1101/2020.03.23.20040501> (2020).
17. Xie, J. & Zhu, Y. Association between ambient temperature and COVID-19 infection in 122 cities from China. *Sci. Total Environ.* **724**, 138201, <https://doi.org/10.1016/J.SCITOTENV.2020.138201> (2020).
18. Tan, J. *et al.* An initial investigation of the association between the SARS outbreak and weather: with the view of the environmental temperature and its variation. *J. Epidemiol. Community Heal.* **59**, 186–192, <https://dx.doi.org/10.1136/jech.2004.020180> (2005).
19. Yuan, J. *et al.* A climatologic investigation of the SARS-CoV outbreak in Beijing, China. *Am. J. Infect. Control* **34**, 234–236, <https://doi.org/10.1016/j.ajic.2005.12.006> (2006).
20. Chan, K. H. *et al.* The effects of temperature and relative humidity on the viability of the SARS coronavirus. *Adv. Virol.* **2011**, <https://doi.org/10.1155/2011/734690> (2011).

21. Wang, J., Tang, K., Feng, K. & Lv, W. High Temperature and High Humidity Reduce the Transmission of COVID-19. *SSRN Electron. J.* <https://doi.org/10.2139/ssrn.3551767> (2020).
22. Metz, J. A. & Finn, A. Influenza and humidity – Why a bit more damp may be good for you! *J. Infect.* **71**, S54–S58, <https://doi.org/10.1016/J.JINF.2015.04.013> (2015).
23. Lowen, A. C., Mubareka, S., Steel, J. & Palese, P. Influenza virus transmission is dependent on relative humidity and temperature. *PLoS Pathog* **3**, e151, <https://doi.org/10.1371/journal.ppat.0030151> (2007).
24. Yang, W. & Marr, L. C. Dynamics of airborne influenza A viruses indoors and dependence on humidity. *PLoS One* **6**, <https://doi.org/10.1371/journal.pone.0021481> (2011).
25. De Jong, J. C., Trouwborst, T. & Winkler, K. C. Mechanisms of inactivation of viruses and macromolecules in air. *Airborne Transm. Airborne Infect.* 124–130 (1973).
26. Moriyama, M., Hugentobler, W. J. & Iwasaki, A. Seasonality of Respiratory Viral Infections. *Annu. Rev. Virol.* <https://doi:10.1146/annurev-virology-012420-022445> (2020).
27. Bukhari, Q. & Jameel, Y. Will Coronavirus Pandemic Diminish by Summer? *SSRN Electron. J.* <https://doi.org/10.2139/ssrn.3556998> (2020).
28. Ellwanger, J. H. & Chies, J. A. B. Wind: a neglected factor in the spread of infectious diseases. *Lancet Planet. Heal.* **2**, e475, [https://doi:10.1016/S2542-5196\(18\)30238-9](https://doi:10.1016/S2542-5196(18)30238-9) (2018).
29. Sarricolea, P., Herrera-Ossandon, M. & Meseguer-Ruiz, Ó. Climatic regionalisation of continental Chile. *J. Maps* **13**, 66–73, <https://doi.org/10.1080/17445647.2016.1259592> (2017).
30. The World Bank. Population density (people per sq. km of land area). Available at: <https://data.worldbank.org/indicator/en.pop.dnst>. Accessed on 22/04/2020 (2020).
31. United Nations. How certain are the United Nations global population projections? Department of Economic and Social Affairs, Population Facts No. 2019/6 (2019).
32. INE. Estimaciones y proyecciones de la población de Chile 2002-2035. Totales regionales, población urbana y rural. Síntesis de resultados Instituto Nacional de Estadísticas Junio 2019 (2019).
33. Horne, B. D. *et al.* Short-Term Elevation of Fine Particulate Matter Air Pollution and Acute Lower Respiratory Infection. *Am. J. Respir. Crit. Care Med.* **198**, 759–766, <https://doi.org/10.1164/rccm.201709-1883OC> (2018).
34. Xie, J., Teng, J., Fan, Y., Xie, R. & Shen, A. The short-term effects of air pollutants on hospitalizations for respiratory disease in Hefei, China. *Int. J. Biometeorol.* **63**, 315–326, <https://doi.org/10.1007/s00484-018-01665-y> (2019).
35. Xu, Q. *et al.* Fine Particulate Air Pollution and Hospital Emergency Room Visits for Respiratory Disease in Urban Areas in Beijing, China, in 2013. *PLoS One* **11**, e0153099, <https://doi.org/10.1371/journal.pone.0153099> (2016).
36. Phosri, A. *et al.* Effects of ambient air pollution on daily hospital admissions for respiratory and cardiovascular diseases in Bangkok, Thailand. *Sci. Total Environ.* **651**, 1144–1153, <https://doi.org/10.1016/J.SCITOTENV.2018.09.183> (2019).

37. IQAir. World Air Quality Region & City PM2.5 Ranking. (2019).
38. INE. Síntesis de resultados censo 2017. (2018).
39. DGA. Atlas del Agua Chile (2016).
40. INE. Adultos mayores en Chile: ¿Cuántos hay? ¿Dónde viven? ¿Y en qué trabajan? (2020). Available at: <https://www.ine.cl/prensa/detalle-prensa/2020/04/15/adultos-mayores-en-chile-cuántos-hay-dónde-viven-y-en-qué-trabajan>.
41. MINSAL. *Informe epidemiológico Enfermedad por SARS-Cov-2 (COVID-19) CHILE 17-04-2020*. (2020).
42. INIA. Agrometeorología Red Agrometeorológica de Inia. Available at: <https://agrometeorologia.cl/>. Accessed on 17/04/2020 (2020).
43. SINCA-MMA. SINCA Sistema de Información Nacional de Calidad del Aire. Available at: <https://sinca.mma.gob.cl/index.php/>. Accessed on 17/04/2020 (2020).
44. CONAF. Proyecto Catastro y Evaluación de los Recursos Vegetacionales Nativos de Chile. Available at: <http://sit.conaf.cl/>. Accessed on 14/08/2018 (2013).
45. IDE Chile. IDE Chile Infraestructura de Datos Geoespaciales. Available at: <http://www.ide.cl/>. (2020).
46. R Core Team. R: A language and environment for statistical computing. R Foundation for Statistical Computing v. 3.2.5. (2018).
47. Zuur, A., Ieno, E. N., Walker, N., Saveliev, A. A. & Smith, G. M. *Mixed effects models and extensions in ecology with R*. (Springer Science & Business Media, 2009).
48. Pinheiro, J., Bates, D., DebRoy, S. & Sarkar, D. R Core Team (2017) nlme: linear and nonlinear mixed effects models. R package version 3.1-131, <https://CRAN.R-project.org/package=nlme> (2017).

Tables

Table 1. Mean values (standard error) of the variables recorded between February 23 to April 16, 2020 in relation to climates.

	Desert (n=56)	Semiarid (n=64)	Mediterranean (n=624)	Marine South West (n=160)	Tundra (n=64)
Altitude (m a.s.l.)	879.7 (139.3)	429.6 (75.0)	263.3 (8.9)	74.9 (5.2)	84.7 (13.3)
Population size (n° inhabitants)	159,749.1 (19765.6)	112,296.0 (12135.5)	93,203.9 (5005.6)	50,580.2 (5464.0)	34,567.9 (6066.2)
Pop. density (inhabitants km ⁻²)	22.5 (3.6)	48.7 (8.0)	933.7 (101.1)	43.8 (4.6)	2.7 (0.4)
Maximum temperature (°C)	23.9 (0.6)	23.5 (0.4)	24.4 (0.2)	19.1 (0.2)	15.2 (0.4)
Minimum temperature (°C)	11.5 (0.9)	12.3 (0.3)	8.8 (0.1)	8.0 (0.2)	6.8 (0.3)
Mean temperature (°C)	17.7 (0.7)	17.9 (0.2)	16.6 (0.1)	13.5 (0.2)	10.9 (0.3)
Relative humidity (%)	58.9 (1.8)	69.8 (0.9)	62.2 (0.4)	76.7 (0.4)	71.2 (1.1)
Absolute humidity (g m ⁻³)	9.4 (0.5)	10.6 (0.1)	8.9 (0.1)	9.0 (0.1)	7.1 (0.1)
Accumulated precipitation (mm)	0.2 (0.1)	0.0 (0.0)	0.3 (0.0)	2.5 (0.3)	1.3 (0.2)
Atmospheric pressure (mbar)	859.2 (19.8)	984.2 (3.5)	967.4 (3.2)	1002.4 (1.2)	986.6 (1.9)
Solar radiation (Mj m ⁻²)	30.1 (1.6)	23.8 (1.4)	24.1 (0.5)	15.7 (0.5)	12.8 (0.6)
Wind speed (km h ⁻¹)	5.3 (0.6)	6.2 (0.3)	5.6 (0.1)	5.3 (0.2)	10.5 (0.8)
MP2.5 (µg m ⁻³)	8.3 (0.4)	8.5 (0.3)	14.9 (0.3)	15.4 (1.1)	10.8 (1.2)
MP10 (µg m ⁻³)	27.2 (0.6)	25.7 (0.7)	42.5 (0.8)	24.2 (1.3)	26.0 (.1)
Absolute infection (infected week ⁻¹)	6.8 (2.8)	1.3 (0.3)	5.8 (1.3)	3.3 (1.6)	7.9 (7.3)
Relative infection (infected week / n° inhabitants)	0.012 (0.007)	0.003 (0.001)	0.044 (0.037)	0.005 (0.001)	0.024 (0.014)

Table 2. Results of the best linear models (after backward model selection procedure) explaining the influence of environmental predictors on absolute and relative COVID-19 infection rates. Total degrees of freedom from models are, respectively, 120 and 118.

	Estimate	SE	t-value	<i>P</i>
<i>Absolute COVID-19 infection rates</i>				
Intercept	5.08	0.67		
Mean temperature (MT)	-0.99	0.17	-5.74	< 0.0001
Population size	7.09	1.03	6.83	< 0.0001
Relative humidity	-0.59	0.11	-5.50	< 0.0001
Wind speed (WS)	0.50	0.12	4.04	0.0001
MT x WS	0.23	0.09	2.57	0.0116
<i>Relative COVID-19 infection rates</i>				
Intercept	0.0562	0.0006		
Mean temperature (MT)	-0.0013	0.0007	-2.01	0.0462
Relative humidity	-0.0006	0.0006	-1.02	0.3089

Figures

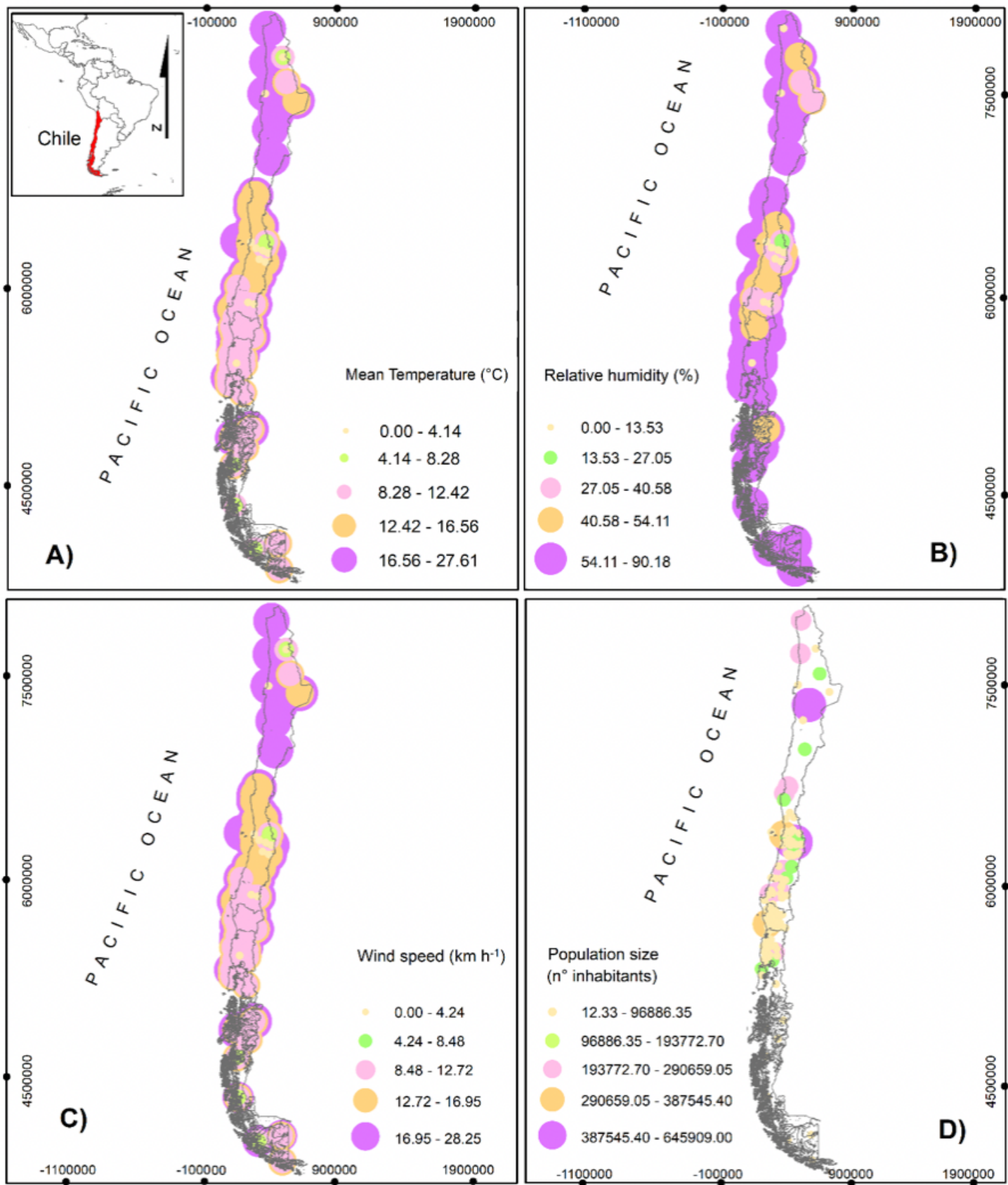


Figure 1

Map of Chilean distribution of (A) mean temperature ($^{\circ}\text{C}$), (B) relative humidity (%), (C) wind speed (km h^{-1}) and (D) population size (n° inhabitants).

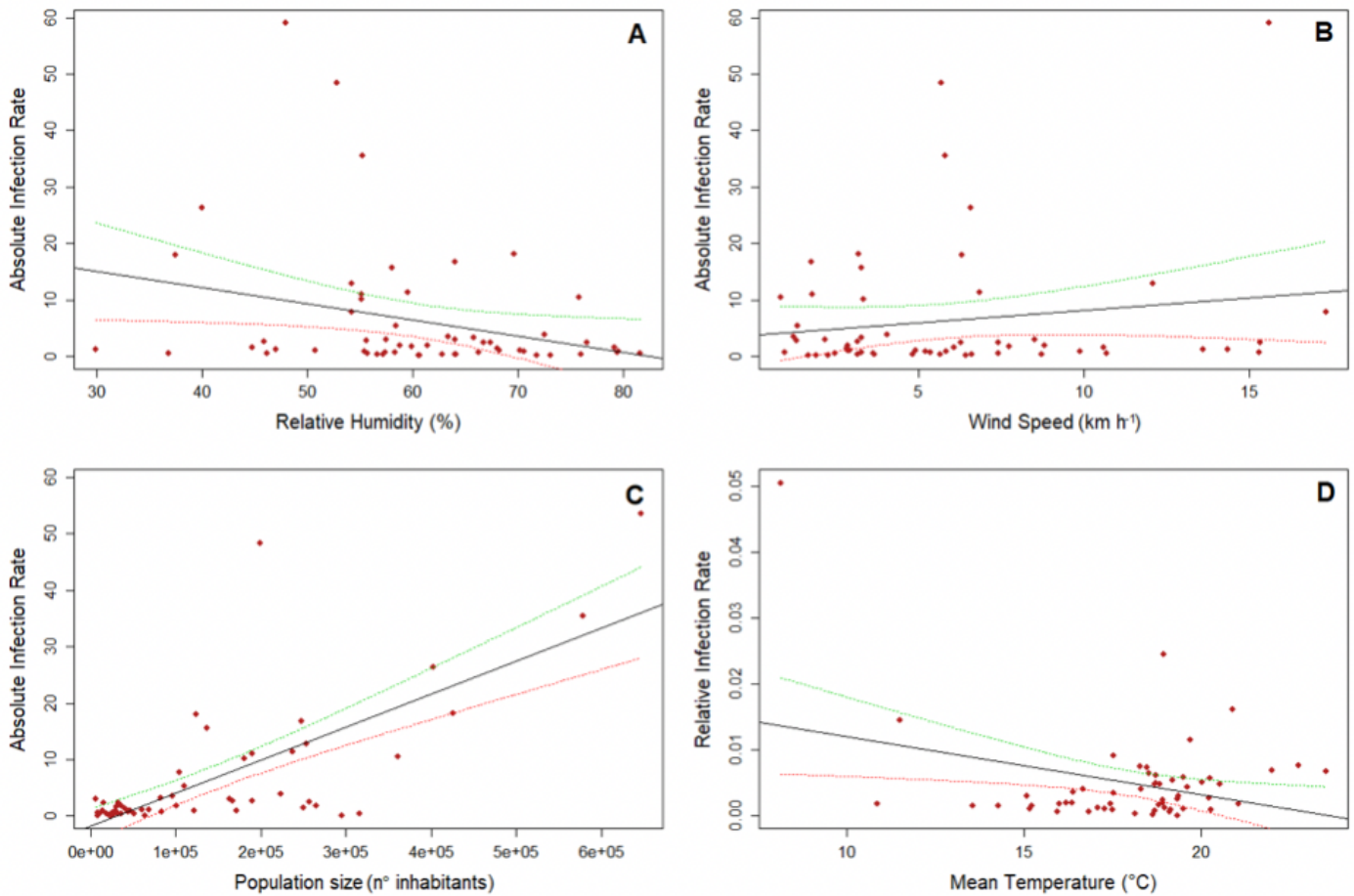


Figure 2

Scatter plots between absolute infection rate (number of infected inhabitants per week) and relative humidity (%; A), wind speed (km h^{-1} ; B) and population size (n° inhabitants; C). Between relative infection rate (the former variable divided by population size) and mean temperature ($^{\circ}\text{C}$; D).

Supplementary Files

This is a list of supplementary files associated with this preprint. Click to download.

- [SupplementaryTableS1Ms.CorreaAranedaEtAl.xlsx](#)
- [SupplementaryTableS2Ms.CorreaAranedaEtAl.pdf](#)
- [GraphicalAbstract.png](#)